SPONSORED BY R&D SYSTEMS INC.

www.rndsystems.com/pathways

Palladium-Catalyzed Aerobic Dehydrogenation of Substituted Cyclohexanones to Phenols

Yusuke Izawa *et al.*

Science **333**, 209 (2011);
DOI: 10.1126/science.1204183

This copy is for your personal, non-commercial use only.

If you wish to distribute this article to others, you can order high-quality copies for your colleagues, clients, or customers by clicking here.

Permission to republish or repurpose articles or portions of articles can be obtained by following the guidelines here.

The following resources related to this article are available online at www.sciencemag.org (this information is current as of November 19, 2012):

Updated information and services, including high-resolution figures, can be found in the online version of this article at:
http://www.sciencemag.org/content/333/6039/209.full.html

Supporting Online Material can be found at:
http://www.sciencemag.org/content/suppl/2011/06/08/science.1204183.DC1.html

This article **cites 40 articles**, 1 of which can be accessed free:
http://www.sciencemag.org/content/333/6039/209.full.html#ref-list-1

This article appears in the following **subject collections:**
Chemistry
http://www.sciencemag.org/cgi/collection/chemistry

Downloaded from www.sciencemag.org on November 19, 2012

Science (print ISSN 0036-8075; online ISSN 1095-9203) is published weekly, except the last week in December, by the American Association for the Advancement of Science, 1200 New York Avenue NW, Washington, DC 20005. Copyright 2011 by the American Association for the Advancement of Science; all rights reserved. The title *Science* is a registered trademark of AAAS.

tional period, which is on the order of picoseconds. E_s between high- and low-chalcocite phases results from the different Cu arrangements in these two phases and the related extra Ewald energy at the interface. This is similar to the case of the interface between wurtzite (WZ) and zincblende (ZB), where the different second nearest-neighbor atomic positions cause different Ewald energies in these two phases. It has been found that the interface energy between WZ and ZB per surface unit cell is similar to the energy difference per unit cell (*28*). Thus, if we take this approximation that the interface energy between low- and high-chalcocite is the same as the internal energy difference between these two phases, $(\varepsilon_1 - \varepsilon_2) = 40$ meV per unit cell (*23*), and assume that there are N Cu_2S unit formulae inside a spherical core, we have $E_s = (36\pi)^{1/3}N^{2/3}(\varepsilon_1 - \varepsilon_2)$. Note that $C = C_{unit}N$, and $C_{unit} = 52$ J/mol·K (*23*). Thus, from Eq. 3, we get $\tau \sim 2$ s when $N = 1000$ and $\tau_0 = 1$ ps (*29*). This fluctuation time is of the same order as our observed experimental value.

In summary, we have observed dynamic structural transformations of a single Cu_2S nanorod from a low- to a high-chalcocite structure. The influence of the surface and interface energies on nucleation and pinning phenomena of a particular phase by defects suggests strategies for stabilizing metastable structures. The ability to directly visualize these processes will aid in the future design of materials with new and controlled phases.

References and Notes

1. M. H. R. Lankhorst, B. W. S. M. M. Ketelaars, R. A. M. Wolters, *Nat. Mater.* **4**, 347 (2005).
2. S. H. Lee, Y. Jung, R. Agarwal, *Nat. Nanotechnol.* **2**, 626 (2007).
3. J. Christian, *The Theory of Transformations in Metals and Alloys* (Pergamon, London, 1965).
4. H. E. Stanley, *Introduction to Phase Transitions and Critical Phenomena* (Oxford Univ. Press, New York, 1987).
5. M. S. S. Challa, D. P. Landau, K. Binder, *Phase Transit.* **24**, 343 (1990).
6. K. Jacobs, D. Zaziski, E. C. Scher, A. B. Herhold, A. Paul Alivisatos, *Science* **293**, 1803 (2001).
7. Q. X. Guo *et al.*, *Nano Lett.* **8**, 972 (2008).
8. R. F. Smith *et al.*, *Phys. Rev. Lett.* **101**, 065701 (2008).
9. J. S. Wittenberg, M. G. Merkle, A. P. Alivisatos, *Phys. Rev. Lett.* **103**, 125701 (2009).
10. Z. W. Wang *et al.*, *Proc. Natl. Acad. Sci. U.S.A.* **107**, 17119 (2010).
11. M. Lentzen, *Microsc. Microanal.* **14**, 16 (2008).
12. C. Ö. Girit *et al.*, *Science* **323**, 1705 (2009).
13. R. Erni *et al.*, *Phys. Rev. B* **82**, 165443 (2010).
14. B. Sadtler *et al.*, *J. Am. Chem. Soc.* **131**, 5285 (2009).
15. H. T. Evans, *Nat. Phys. Sci.* **232**, 69 (1971).
16. M. J. Buerger, B. J. Wuensch, *Science* **141**, 276 (1963).
17. A. Putnis, *Am. Mineral.* **62**, 107 (1977).
18. Supporting material is available on *Science* Online.
19. T. Yokota, M. Murayama, J. M. Howe, *Phys. Rev. Lett.* **91**, 265504 (2003).
20. R. F. Egerton, P. Li, M. Malac, *Micron* **35**, 399 (2004).
21. A. Reguer *et al.*, *Ultramicroscopy* **110**, 61 (2009).
22. M. S. S. Challa, D. P. Landau, K. Binder, *Phys. Rev. B* **34**, 1841 (1986).
23. D. J. Chakrabarti, D. E. Laughlin, *J. Phase Equil.* **4**, 254 (1983).
24. www.totalresolution.com
25. R. W. Potter, *Econ. Geol.* **72**, 1524 (1977).
26. S. L. Lai, J. Y. Guo, V. Petrova V, G. Ramanath, L. H. Allen, *Phys. Rev. Lett.* **77**, 99 (1996).
27. L. D. Landau, E. M. Lifshitz, *Statistical Physics* (Pergamon, New York, 1980).
28. F. Glas, *J. Appl. Phys.* **104**, 093520 (2008).
29. A. F. Voter, *Phys. Rev. B* **34**, 6819 (1986).

Acknowledgments: We thank U. Dahmen at National Center for Electron Microscopy (NCEM) and E. Borrero and C. Dellago at University of Vienna for helpful discussions. The authors are grateful to the support of Helios Solar Energy Research Center (SERC) and NCEM, which are funded by the director of the Office of Science, Office of Basic Energy Sciences (BES), Materials Science and Engineering Division of the U.S. Department of Energy (DOE) under contract no. DE-AC02-05CH11231. TEM experiments were performed using TEAM0.5 microscope at NCEM. X-ray experiments were performed at the Stanford Synchrotron Radiation Laboratory, a DOE-BES user facility. J.B.R. was funded by a fellowship from Intel Corporation, and T.A.M. and A.L. were supported by the DOE BES Materials Sciences and Engineering Division. H.Z. conceived the work and performed the experiments; H.Z. and A.P.A. analyzed the data and wrote the paper; J.B.R. prepared nanorod samples, took ensemble x-ray data, and edited the paper; B.S. contributed to nanorod sample preparation and edited the paper; M.F.T., A.L., and T.A.M. provided x-ray analysis infrastructure; L.-W.W. provided theoretical calculation and edited the paper; and C.K. contributed to image analysis and edited the paper.

Supporting Online Material

www.sciencemag.org/cgi/content/full/333/6039/206/DC1
Materials and Methods
SOM Text
Figs. S1 to S4
Table S1
References (*30*–*35*)
Movies S1 to S6

23 February 2011; accepted 25 May 2011
10.1126/science.1204713

Palladium-Catalyzed Aerobic Dehydrogenation of Substituted Cyclohexanones to Phenols

Yusuke Izawa, Doris Pun, Shannon S. Stahl*

Aromatic molecules are key constituents of many pharmaceuticals, electronic materials, and commodity plastics. The utility of these molecules directly reflects the identity and pattern of substituents on the aromatic ring. Here, we report a palladium(II) catalyst system, incorporating an unconventional *ortho*-dimethylaminopyridine ligand, for the conversion of substituted cyclohexanones to the corresponding phenols. The reaction proceeds via successive dehydrogenation of two saturated carbon-carbon bonds of the six-membered ring and uses molecular oxygen as the hydrogen acceptor. This reactivity demonstrates a versatile and efficient strategy for the synthesis of substituted aromatic molecules with fundamentally different selectivity constraints from the numerous known synthetic methods that rely on substitution of a preexisting aromatic ring.

Phenols are common precursors and core structures of industrial chemicals ranging from pharmaceuticals to polymers. The introduction of chemical functional groups with specific patterns around the aromatic ring represents a key challenge in the preparation of these molecules (*1*). Electrophilic aromatic substitutions are classical chemical reactions that remain among the most versatile methods for the synthesis of substituted phenols; however, strong electronic directing effects associated with these reactions limit their utility to the preparation of ortho- and para-substituted derivatives. This limitation has inspired extensive efforts to identify complementary routes to substituted phenols, such as a recent two-step arene C–H borylation/oxidation procedure for the introduction of a hydroxyl group into an aromatic ring, guided by steric rather than electronic effects (*2*). Recent advances in palladium-catalyzed aerobic oxidation reactions (*3*–*5*) suggested to us that diverse phenol derivatives, including those with meta substitution, could be accessed by dehydrogenation of cyclohexanones via sequential Pd-mediated C–H activation/β-hydride elimination steps, followed by tautomerization of the resulting dienone product (Fig. 1A). This strategy is appealing because Pd^{II}–hydride intermediates formed in this mechanism could be oxidized by molecular oxygen (*6*, *7*), thereby enabling the overall process to be catalytic in Pd with water as the sole by-product (Fig. 1B). Successful catalysts for this class of reactions could find broad utility owing to the numerous straightforward chemical reactions that provide access to substituted cyclohexanones, including enolate arylation and alkylation methods, conjugate addition to cyclohexenones, and Robinson annulation and Diels-Alder reactions (Fig. 1C).

The preparation of phenols from ketone precursors have been explored previously (*8*–*16*). Condensation reactions of acyclic ketones, for example, with β-ketoaldehydes or β-diketones, enable direct access to substituted phenols (*8*), but low product yields, limited access to starting materials, and/or formation of isomeric products

Department of Chemistry, University of Wisconsin–Madison, 1101 University Avenue, Madison, WI 53706, USA.

*To whom correspondence should be addressed. E-mail: stahl@chem.wisc.edu

Downloaded from www.sciencemag.org on November 19, 2012

have restricted the utility of these procedures. Methods for formation of phenols via dehydrogenation of cyclohexenones have been pursued (*8*–*13*), but reactions of this type typically use undesirable stoichiometric reagents, such as DDQ (2,3-dichloro-5,6-dicyano-1,4-benzoquinone) (*17*); use stepwise procedures, such as bromination/dehydrobromination; or require harsh reaction conditions (≥200°C) that limit functional group compatibility. In contrast, no effective methods for dehydrogenation of substituted cyclohexanones exist, with relevant precedents almost exclusively limited to reactions of unsubstituted cyclohexanone and yields of ≤30% (mostly <5%) (*12*–*16*). Iridium complexes bearing tridentate "pincer" ligands are among the most effective catalysts for the dehydrogenation of saturated hydrocarbons (*18*, *19*). These reactions are typically carried out in the presence of a sacrificial hydrogen acceptor, such as norbornene or *tert*-butylethylene, and a recent investigation of the reaction of an Ir-pincer complex with cyclohexanone resulted in stoichiometric dehydrogenation. Catalytic turnover was inhibited by the formation of an Ir-phenoxide product, (pincer)Ir(H)(OPh) (*20*).

In order to explore prospects for the proposed Pd-catalyzed dehydrogenation methods, we investigated the reactivity of 3-methylcyclohexenone (**1a**) and 3-methylcyclohexanone (**1b**) under 1 atm of O_2 with various Pd^{II} catalysts. Preliminary analysis of Pd^{II} sources, solvents, and reaction conditions revealed that 3-methylphenol (*meta*-cresol) could be obtained in modest yields from **1a** and **1b** (28 to 52%) with 3 mol % $Pd(OAc)_2$ or $Pd(TFA)_2$ (OAc is an acetate group and TFA is trifluoroacetate) in dimethylsulfoxide (DMSO) as the solvent under 1 atm of O_2 at 80°C (Fig. 2, entries 1 and 2) (*21*, *22*). Brønsted bases, such as sodium acetate, and traditional monodentate and bidentate nitrogen ligands (pyridine, bipyridine, and phenanthroline) failed to increase the yield of the phenol product (entries 3 to 6; for expanded screening results, see table S2). The use of 4,5-diazafluorenone (*23*) led to a substantial increase in the yield of *m*-cresol from **1a** (78%, entry 7); however, conversion to phenol from the saturated cyclohexanone **1b** was still unsatisfactory. Both key steps in the substrate oxidation sequence, C–H activation and β-hydride elimination (Fig. 1A), should benefit from a more electrophilic catalyst, and recent success with 2-fluoropyridine (^{2F}py) as an electron-deficient ligand in aerobic oxidative coupling reactions (*24*) prompted us to evaluate ligands of this type in the dehydrogenation reactions (entries 8 to 15). The use of ^{2F}py as a ligand led to a modest improvement in the yield of **2** from **1b** (44%, entry 10); however, the best results were obtained when 2-(*N*,*N*-dimethylamino) pyridine (^{2NMe2}py) was used in combination with *p*-toluenesulfonic acid (TsOH) (entry 18). We speculate that the improved results obtained with the ^{2NMe2}py/TsOH combination relative to those with ^{2NMe2}py alone (compare entries 15 and 18) reflect the ability of TsOH to protonate the tertiary amine of the coordinated pyridine and thereby afford a more electron-deficient pyridine ligand. The position of the dimethylamino group on the pyridine ligand is important, as revealed by the inferior results obtained with 4-(*N*,*N*-dimethylamino)pyridine in place of the 2-substituted ligand (entries 19 and 20). Common heterogeneous palladium catalysts failed to afford the desired *m*-cresol (entries 21 to 24).

The optimized catalytic conditions (Fig. 2, entry 18) proved to be effective in the preparation of a number of substituted phenol derivatives (Fig. 3). Varying the position of the methyl substituent on the cyclohexanone had little effect on the outcome of the reaction; the corresponding *ortho*-, *meta*-, and *para*-cresols were each obtained in good yield (Fig. 3 entries 1 to 3). Aryl-substituted phenols, including a number of meta-substituted derivatives, were accessed via the dehydrogenation of the corresponding arylcyclohexanone derivatives (entries 4 to 11). The 3-arylcyclohexanones were readily obtained via conjugate addition of aryl boronic acids to cyclohexenone, and both electron-donating and electron-withdrawing groups were tolerated in the dehydrogenation reaction. Substrates with aryl groups bearing a *para* bromide or iodide afforded only low yields of the desired phenol (28% and 16%, respectively; not shown in Fig. 3). Diels-Alder cycloaddition and Robinson annulation represent classical and widely used synthetic organic reactions that provide efficient routes to cyclohexenones bearing multiple substituents on the six-membered ring. The aerobic oxidation method described here provides an attractive alternative to the use of stoichiometric reagents, such as DDQ, which have been used previously in the dehydrogenation of cyclohexenones (*17*), and such substrates underwent very effective dehydrogenation under the optimized catalytic conditions, including those bearing alkyl, aryl, and/or ester substituents (entries 12 to 17).

The 3,5-disubstituted cyclohexenones were pursued further, because the corresponding phenol derivatives exhibit important biological activity and products of this type cannot be readily prepared by classical aromatic-substitution, metal-catalyzed cross-coupling, or related synthetic methods. As a representative example, *O*-terphenylcarbamate **5** was recently identified as a potent in vitro allosteric inhibitor of the human luteinizing hormone

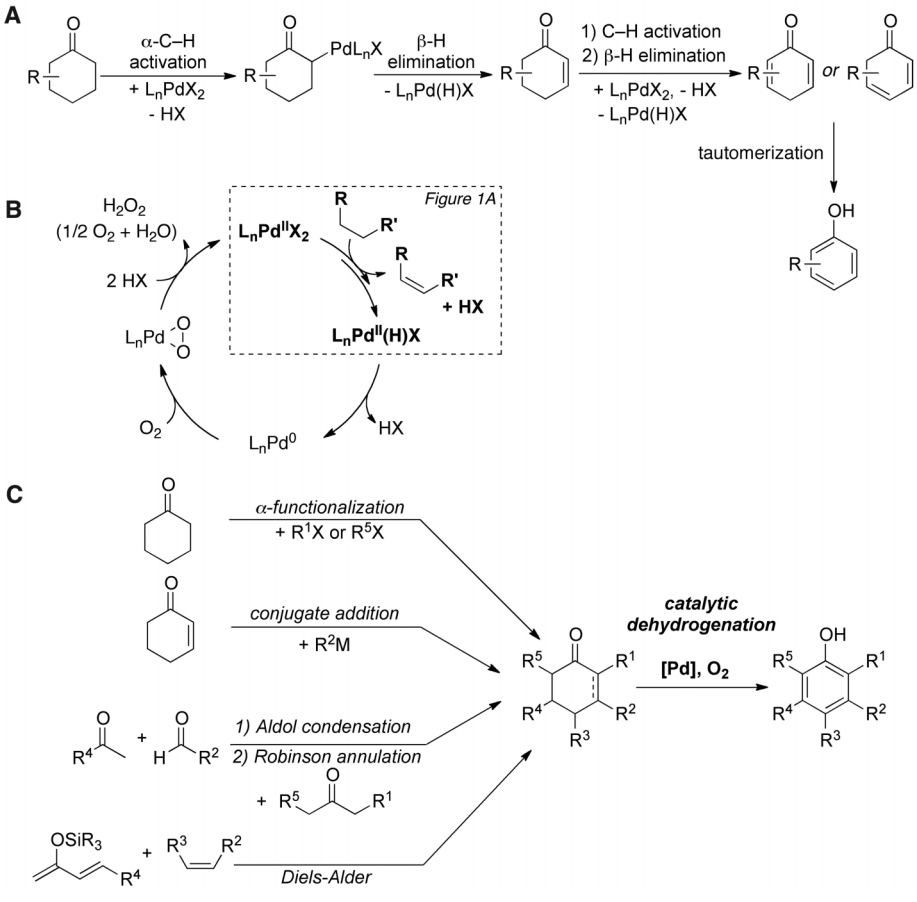

Fig. 1. Strategy for the synthesis of phenols via aerobic oxidative dehydrogenation of cyclohexanone derivatives. (**A**) Stepwise sequence for Pd-mediated dehydrogenation of cyclohexanone. (**B**) Catalytic mechanism whereby cyclohexanone dehydrogenation can be achieved with O_2 as the terminal oxidant. (**C**) Representative synthetic methods that afford facile access to substituted cyclohexanone derivatives. L, a ligand; M, metal; R, organic substituent; X, halide or pseudohalide.

Downloaded from www.sciencemag.org on November 19, 2012

receptor, which has been implicated in fertility and ovarian cancer (*25*). This compound was prepared by traditional Suzuki coupling methods using 3,5-dibromophenol as the starting material; however, introduction of the unsymmetrical aryl substitution pattern results in low yields of the biaryl intermediate **6** and the desired 3,5-diarylphenol **4** (30% and 62% yields, respectively; Fig. 4). In contrast, the 3,5-diarylcyclohexenone

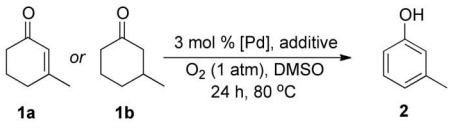

entry	catalyst/ligand/additive	reagent: 1a	1b
		Yield of *m*-cresol (%)	
1	$Pd(OAc)_2$	30	40
2	$Pd(TFA)_2$	52	28
3	$Pd(TFA)_2$/NaOAc (1 equiv)	13	21
4	$Pd(TFA)_2$/pyridine (6%)	39	16
5	$Pd(TFA)_2$/bipyridine (3%)	26	18
6	$Pd(TFA)_2$/phenanthroline (3%)	15	18
7	$Pd(TFA)_2$/4,5-diazafluorenone (3%)	78	25
8	$Pd(TFA)_2/^{3CO2Et}py$ (6%)	60	14
9	$Pd(TFA)_2/^{3NO2}py$ (6%)	64	24
10	$Pd(TFA)_2/^{2F}py$ (6%)	59	44
11	$Pd(TFA)_2/^{2OH}py$ (6%)	68	32
12	$Pd(TFA)_2/^{2OMe}py$ (6%)	64	24
13	$Pd(TFA)_2/^{2NH2}py$ (6%)	65	8
14	$Pd(TFA)_2/^{2NHMe}py$ (6%)	72	22
15	$Pd(TFA)_2/^{2NMe2}py$ (6%)	53	24
16	$Pd(TFA)_2/^{2NH2}py$ (6%)/TsOH (12%)	65	45
17	$Pd(TFA)_2/^{2NHMe}py$ (6%)/TsOH (12%)	70	65
18	**$Pd(TFA)_2/^{2NMe2}py$ (6%)/TsOH (12%)**	**74 (100)†**	**79 (84)†**
19	$Pd(TFA)_2/^{4NMe2}py$ (6%)	57	55
20	$Pd(TFA)_2/^{4NMe2}py$ (6%)/TsOH (12%)	68	28
21	Pd/C	1.5	< 1
22	Pd/Al_2O_3	< 1	0
23	$Pd/CaCO_3$	0	0
24	$Pd(OH)_2/C$	0	0

†Yield in parentheses based on 5 mol % Pd.

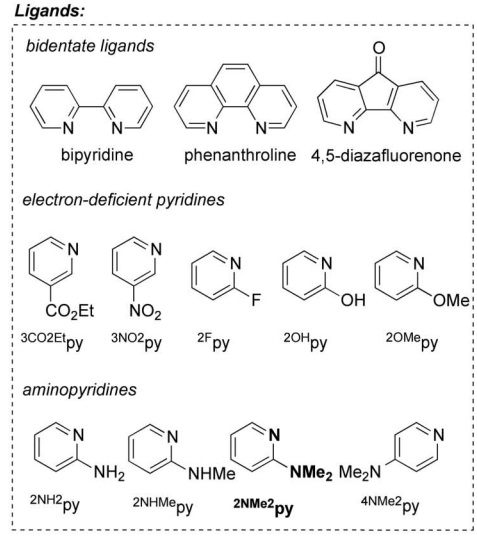

Fig. 2. Catalyst optimization for aerobic oxidative dehydrogenation of cyclohexanone derivatives **1a** and **1b**. Reaction conditions are as follows: cyclic ketone (1.0 mmol), PdX_2 (0.03 mmol), ligand/TsOH (mol % indicated), DMSO (0.4 ml), 80°C, 1 atm O_2, 24 hours. Et, ethyl group; Me, methyl group; TsOH, *p*-toluenesulfonic acid. Yields determined by gas chromatography.

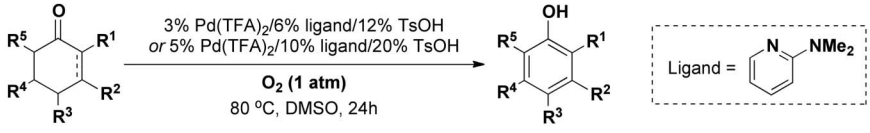

entry	substrate	phenol	% yield
1	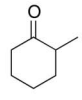	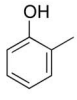	70*
2	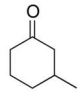	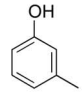	76*
3	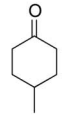	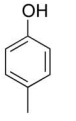	86*
4	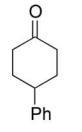	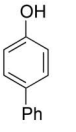	83*
5	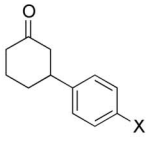	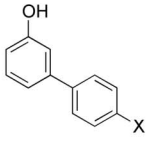	X = H 78*
6			Ph 85†
7			OMe 96*
8			CF_3 93*
9			CO_2Me 75†
10			F 65†
11			Cl 57†
12	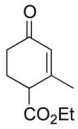	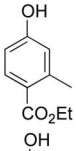	79†
13		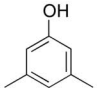	76*
14	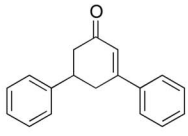	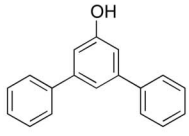	95†
15	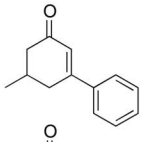	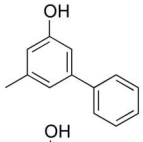	73†
16	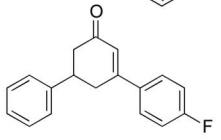	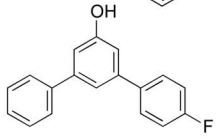	91†
17	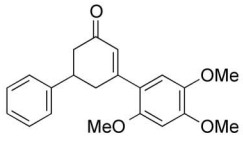	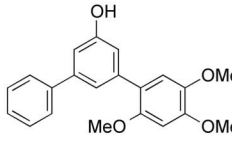	85†

* 3% Pd/6% ligand/12% TsOH. † 5% Pd/10% ligand/20% TsOH.

Fig. 3. Palladium-catalyzed aerobic dehydrogenation of cyclic ketones. Reaction conditions are as follows: cyclic ketone (1.0 mmol), $Pd(TFA)_2$ (0.03 or 0.05 mmol), 2-(*N*,*N*-dimethylamino)pyridine (0.06 or 0.10 mmol), TsOH (0.12 or 0.20 mmol), DMSO (0.4 ml), 1 atm O_2, 80°C, 24 hours. Isolated product yields are reported.

Downloaded from www.sciencemag.org on November 19, 2012

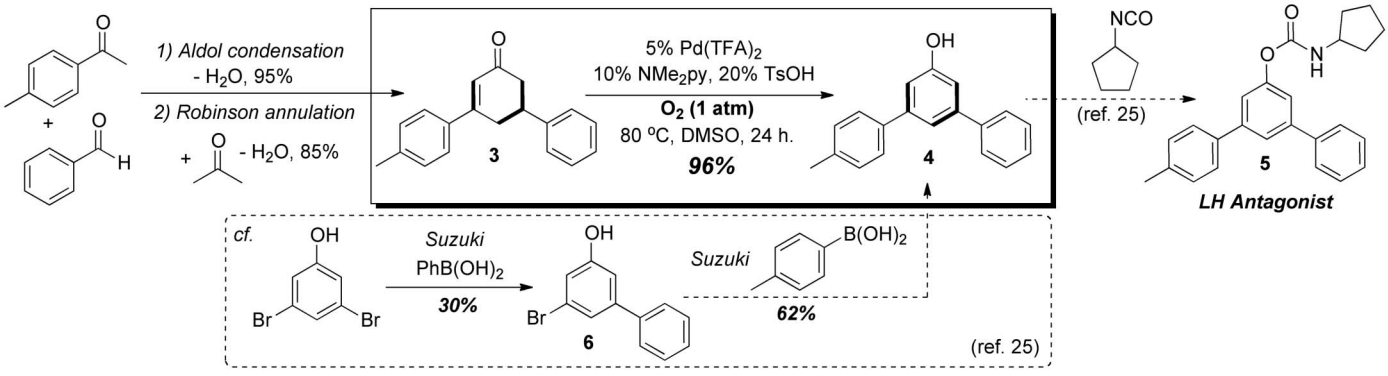

Fig. 4. Application of palladium-catalyzed aerobic oxidative dehydrogenation in the preparation of a terphenyl-derived allosteric inhibitor of the luteinizing hormone receptor. Ph, phenyl group.

derivative **3** is obtained readily from very inexpensive starting materials (4-methylacetophenone, benzaldehyde, and acetone) via sequential aldol condensation and Robinson annulation. Subsequent Pd-catalyzed dehydrogenation of **3** afforded phenol **4** in excellent yield.

Preliminary mechanistic analysis of these dehydrogenation reactions was performed by monitoring the conversion of cyclohexanone to phenol by gas chromatography. The kinetic time course revealed the formation and disappearance of the partially dehydrogenated intermediate, cyclohexenone (Fig. 5A). This result is consistent with the overall catalytic mechanism in Fig. 1B, in which the substrate dissociates from the catalyst after each dehydrogenation step. A fit of the kinetic data based on a simple sequential reaction model reveals that the two dehydrogenation steps have similar rate constants, $k_1 = 0.12(\pm0.02)$ hour^{-1} and $k_2 = 0.33(\pm0.04)$ hour^{-1} (Fig. 5B). The dehydrogenation of cyclohexenone, monitored independently, exhibits a rate constant somewhat lower than that obtained from the fit of the sequential reaction, $k_2' = 0.19(\pm0.02)$ hour^{-1}. Accurate interpretation of these results will require further investigation; however, the higher concentration of cyclohexenone in the latter reaction may slow the catalytic turnover via alkene coordination to Pd.

The joint application of catalyst screening and mechanistic studies will play an important role in extending these reactions to different product classes. For example, catalysts that can effect the first step substantially more rapidly than the second step (k_1:k_2 > 10:1) would enable selective formation of the enone products rather than phenols. Moreover, it should be possible to develop efficient catalysts for dehydrogenative aromatization of other substrate classes, such as substituted cyclohexenes (*26*–*28*). Substrates of this type are readily accessed via Diels-Alder cycloaddition reactions, and their dehydrogenation could proceed via sequential allylic C–H activation/β-hydride elimination steps (Fig. 5C). Toward this end, preliminary studies reveal that cyclohexene derivative **7** undergoes efficient dehydrogenation to the trisubstituted arene **8** in near-quantitative yield.

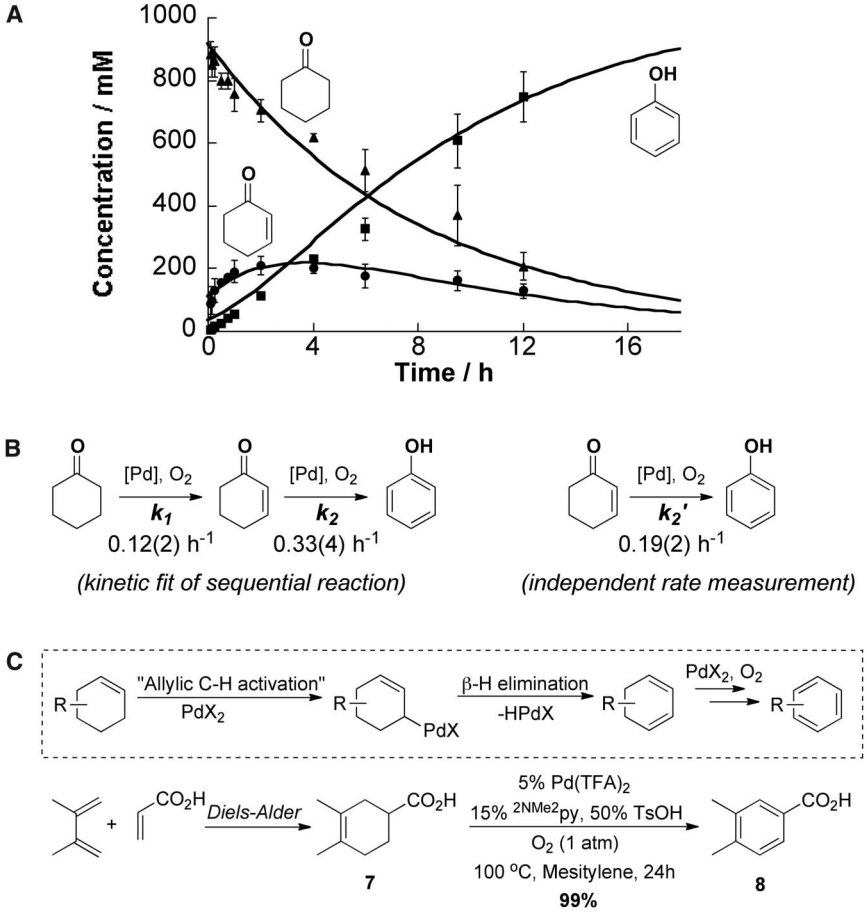

Fig. 5. (**A**) Kinetic profile of Pd^{II}-catalyzed aerobic dehydrogenation of cyclohexanone and cyclohexenone, showing the formation and decay of cyclohexenone as an intermediate in the reaction. Reaction conditions are as follows: cyclohexanone (0.5 mmol), $Pd(TFA)_2$ (0.025 mmol), 2-(*N*,*N*-dimethylamino)pyridine (0.05 mmol), TsOH (0.10 mmol), DMSO (0.5 ml), 1 atm O_2, 80°C. Error bars represent standard deviations from five independent measurements. (**B**) Comparison of the rate constants obtained for the dehydrogenation steps in the sequential conversion of cyclohexanone to phenol and in the direct dehydrogenation of cyclohexenone. (**C**) General strategy and a specific example of Pd-catalyzed aerobic dehydrogenation of cyclohexenes.

Methods for selective dehydrogenation of saturated carbon-carbon bonds represent an important class of C–H functionalization (*18*, *29*), and the reactions presented above highlight the prospective utility of such methods in the synthesis of substituted aromatic molecules. These reactions achieve high conversions and product yields, they are capable of using O_2 as the hydrogen acceptor,

Downloaded from www.sciencemag.org on November 19, 2012

and the catalyst tolerates useful substrate functional groups, including aromatic and heteroatom substituents. With the development of improved methods for safe and scalable aerobic oxidation reactions (*30*), dehydrogenation methods of this type could have an important impact on laboratory- and industrial-scale chemical synthesis.

References and Notes

1. J. H. P. Tyman, *Synthetic and Natural Phenols* (Elsevier, New York, 1996).
2. R. E. Maleczka Jr., F. Shi, D. Holmes, M. R. Smith 3rd, *J. Am. Chem. Soc.* **125**, 7792 (2003).
3. S. S. Stahl, *Angew. Chem. Int. Ed.* **43**, 3400 (2004).
4. K. M. Gligorich, M. S. Sigman, *Chem. Commun.* **2009**, 3854 (2009).
5. X. Chen, K. M. Engle, D.-H. Wang, J.-Q. Yu, *Angew. Chem. Int. Ed.* **48**, 5094 (2009).
6. M. M. Konnick, S. S. Stahl, *J. Am. Chem. Soc.* **130**, 5753 (2008).
7. M. C. Denney, N. A. Smythe, K. L. Cetto, R. A. Kemp, K. I. Goldberg, *J. Am. Chem. Soc.* **128**, 2508 (2006).
8. P. Bamfield, P. F. Gordon, *Chem. Soc. Rev.* **13**, 441 (1984).
9. E. C. Horning, M. G. Horning, *J. Am. Chem. Soc.* **69**, 1359 (1947).
10. P. P. Fu, R. G. Harvey, *Chem. Rev.* **78**, 317 (1978).
11. T. Moriuchi, K. Kikushima, T. Kajikawa, T. Hirao, *Tetrahedron Lett.* **50**, 7385 (2009).
12. C. S. Yi, D. W. Lee, *Organometallics* **28**, 947 (2009).
13. P. F. Schuda, W. A. Price, *J. Org. Chem.* **52**, 1972 (1987).
14. J. Muzart, J. P. Pete, *J. Mol. Catal.* **15**, 373 (1982).
15. T. T. Wenzel, *J. Chem. Soc. Chem. Commun.* **1989**, 932 (1989).
16. J. Muzart, *Eur. J. Org. Chem.* **2010**, 3779 (2010).
17. D. R. Buckle, in *Encyclopedia of Reagents for Organic Synthesis*, D. Crich, Ed. (Wiley, New York, 2010).
18. J. Choi, A. H. R. MacArthur, M. Brookhart, A. S. Goldman, *Chem. Rev.* **111**, 1761 (2011).
19. R. Ahuja *et al.*, *Nat. Chem.* **3**, 167 (2011).
20. X. W. Zhang, D. Y. Wang, T. J. Emge, A. S. Goldman, *Inorg. Chim. Acta* **369**, 253 (2011).
21. R. C. Larock, T. R. Hightower, *J. Org. Chem.* **58**, 5298 (1993).
22. R. A. T. M. van Benthem, H. Hiemstra, J. J. Michels, W. N. Speckamp, *J. Chem. Soc. Chem. Commun.* **1994**, 357 (1994).
23. A. N. Campbell, P. B. White, I. A. Guzei, S. S. Stahl, *J. Am. Chem. Soc.* **132**, 15116 (2010).
24. Y. Izawa, S. S. Stahl, *Adv. Synth. Catal.* **352**, 3223 (2010).
25. L. H. Heitman *et al.*, *J. Med. Chem.* **52**, 2036 (2009).
26. R. A. Sheldon, J. M. Sobczak, *J. Mol. Catal.* **68**, 1 (1991).
27. J. E. Bercaw, N. Hazari, J. A. Labinger, *J. Org. Chem.* **73**, 8654 (2008).
28. J. E. Bercaw, N. Hazari, J. A. Labinger, P. F. Oblad, *Angew. Chem. Int. Ed.* **47**, 9941 (2008).
29. G. E. Dobereiner, R. H. Crabtree, *Chem. Rev.* **110**, 681 (2010).
30. X. Ye, M. D. Johnson, T. Diao, M. H. Yates, S. S. Stahl, *Green Chem.* **12**, 1180 (2010).

Acknowledgments: We are grateful to the NIH (RC1-GM091161), Mitsubishi Chemical Corporation, and NSF (CHE-1041934 to D.P.) for financial support of this work.

Supporting Online Material

www.sciencemag.org/cgi/content/full/science.1204183/DC1
Materials and Methods
Figs. S1 to S20
Tables S1 and S2
Characterization Data of New Compounds
References (*31*–*43*)

11 February 2011; accepted 1 June 2011
Published online 9 June 2011;
10.1126/science.1204183

High Pre-Eruptive Water Contents Preserved in Lunar Melt Inclusions

Erik H. Hauri,[1]* Thomas Weinreich,[2] Alberto E. Saal,[2] Malcolm C. Rutherford,[2] James A. Van Orman[3]

The Moon has long been thought to be highly depleted in volatiles such as water, and indeed published direct measurements of water in lunar volcanic glasses have never exceeded 50 parts per million (ppm). Here, we report in situ measurements of water in lunar melt inclusions; these samples of primitive lunar magma, by virtue of being trapped within olivine crystals before volcanic eruption, did not experience posteruptive degassing. The lunar melt inclusions contain 615 to 1410 ppm water and high correlated amounts of fluorine (50 to 78 ppm), sulfur (612 to 877 ppm), and chlorine (1.5 to 3.0 ppm). These volatile contents are very similar to primitive terrestrial mid-ocean ridge basalts and indicate that some parts of the lunar interior contain as much water as Earth's upper mantle.

The Moon is thought to have formed in a giant impact collision between a Mars-sized object and an early-formed proto-Earth (*1*). Though all of the inner planets, including Earth, are depleted in water and other volatiles when compared with primitive meteorites, the more extreme depletion of volatiles in lunar volcanic rocks has long been taken as key evidence for a giant impact that resulted in high-temperature catastrophic degassing of the material that formed the Moon (*2*, *3*). However, recent work on rapidly quenched lunar volcanic glasses has detected the presence of water dissolved in lunar magmas at concentrations up to 46 parts per million (ppm) (*4*), and water contents of lunar apatite grains from mare basalts are consistent with similarly minor amounts of water in primitive lunar magmas (*5*–*7*). These results indicate that the Moon is not a perfectly anhydrous planetary body and suggest that some fraction of the Moon's observed depletion in highly volatile elements may be the result of magmatic degassing during the eruption of lunar magmas into the near-vacuum of the Moon's surface.

To bypass the process of volcanic degassing, we conducted a search for lunar melt inclusions in Apollo 17 sample 74220, a lunar soil containing ~99% high-Ti volcanic glass beads, the so-called orange glass with 9 to 12 weight % (wt %) TiO_2 (*8*). Melt inclusions are small samples of magma trapped within crystals that grow in the magma before eruption. By virtue of their enclosure within their host crystals, melt inclusions are protected from loss of volatiles by degassing during magma eruption. Melt inclusions have been used for decades to determine pre-eruptive volatile contents of terrestrial magmas from subduction zones (*9*, *10*), hotspots (*11*, *12*), and mid-ocean ridges (*13*, *14*), as well as volatile contents of martian magmas (*15*, *16*). Using standard petrographic methods, we identified nine inclusion-bearing olivine crystals (Fig. 1) and analyzed melt inclusions hosted within (*17*). The measured water contents of the melt inclusions range from 615 ppm to a maximum of 1410 ppm (Fig. 2); these water contents are up to 100 times as high as the water content of the matrix glass surrounding the olivine crystals (6 to 30 ppm H_2O) and the centers of individual volcanic glass beads from the same sample (*4*). The melt inclusions also contain high concentrations of fluorine (50 to 78 ppm), sulfur (612 to 877 ppm), and chlorine (1.5 to 3.0 ppm) that are 2 to 100 times as high as those of the matrix glasses and individual glass beads from this sample (Fig. 3). Volatile contents corrected for postentrapment crystallization are on average 21% lower than the measured concentrations (*17*) and represent the best estimate of the pre-eruptive concentrations of volatiles in the 74220 magma.

There are few descriptions in the literature of melt inclusions contained within olivine from lunar samples, but these existing observations provide important context for the volatile abundances we have observed. Roedder and Weiblen (*18*–*20*) noted the presence of silicate melt inclusions in the first samples returned from the Apollo 11, Apollo 12, and Luna 16 missions and reported that many primary melt inclusions contained a vapor bubble, requiring dissolved volatiles to have been present in the melt at the time it was trapped within the host crystal. Klein and Rutherford (*21*) and Weitz *et al.* (*22*) found sulfur contents of 600 to 800 ppm, similar to our

[1]Department of Terrestrial Magnetism, Carnegie Institution of Washington, Washington, DC 20015, USA. [2]Department of Geological Sciences, Brown University, Providence, RI 02912, USA. [3]Department of Geological Sciences, Case Western Reserve University, Cleveland, OH 44106, USA.

*To whom correspondence should be addressed. E-mail: ehauri@ciw.edu

Downloaded from www.sciencemag.org on November 19, 2012